Protein Science (1996), 5:1215–1228. Cambridge University Press. Printed in the USA.

Target recognition by calmodulin: Dissecting the kinetics and affinity of interaction using short peptide sequences

P.M. BAYLEY, W.A. FINDLAY,[1] AND S.R. MARTIN

Division of Physical Biochemistry, National Institute for Medical Research, Mill Hill, London NW7 1AA, United Kingdom

(RECEIVED January 17, 1996; ACCEPTED April 5, 1996)

Abstract

The interaction between calmodulin (CaM) and peptide M13, its target binding sequence from skeletal muscle myosin light chain kinase, involves predominantly two sets of interactions, between the N-terminal target residues and the C-domain of calmodulin, and between the C-terminal target residues and the N-domain of calmodulin (Ikura M et al., 1992, *Science 256*:632–638). Using short synthetic peptides based on the two halves of the target sequence, the interactions with calmodulin and its separate C-domain have been studied by fluorescence and CD spectroscopy, calcium binding, and kinetic techniques. Peptide WF10 (residues 1–10 of M13) binds to CaM with $K_d \approx 1\ \mu M$; peptide FW10 (residues 9–18 of M13, with Phe-17 → Trp substitution) binds to CaM with $K_d \approx 100\ \mu M$. The effect of peptide WF10 on calcium binding to calmodulin produces a biphasic saturation curve, with marked enhancement of affinity for the binding of two calcium ions to the C-domain, forming a stable half-saturated complex, Ca_2–CaM–peptide, and confirming the functional importance of the interaction of this sequence with the C-domain. Stopped-flow studies show that the EGTA-induced dissociation of WF10 from Ca_4–CaM proceeds by a reversible relaxation mechanism from a kinetic intermediate state, also involving half-saturation of CaM, and the same mechanism is evident for the full target peptide. Interaction of the N-terminal target residues with the C-domain is energetically the most important component, but interaction of calmodulin with the whole target sequence is necessary to induce the full cooperative interaction of the two contiguous elements of the target sequence with both N- and C-domains of calmodulin. Thus, the interaction of calmodulin with the M13 sequence can be dissected on both a structural and kinetic basis into partial reactions involving intermediates comprising distinct regions of the target sequence. We propose a general mechanism for the calcium regulation of calmodulin-dependent enzyme activation, involving an intermediate complex formed by interaction of the calmodulin C-domain and the corresponding part of the target sequence. This intermediate species can function to regulate the overall calcium sensitivity of activation and to determine the affinity of the calmodulin target interaction.

Keywords: calcium; calmodulin; CD; domains; mechanism; myosin light chain kinase; peptides; stopped-flow

Calmodulin (CaM) is responsible for the calcium-dependent regulation of a number of different eukaryotic enzymes in a variety of cellular locations. This small acidic protein has two domains, each comprising two helix-loop-helix calcium-binding motifs connected by a short antiparallel β-sheet between the two loops (Babu et al., 1985, 1988; Taylor et al., 1991; Rao et al., 1993; Ban et al., 1994). Calcium binding induces significant conformational changes that cause exposure of hydrophobic surfaces on each domain. These changes are shown by recent NMR studies of apo-calmodulin to involve a marked decrease in protein dynamics and re-orientation of calmodulin α-helices on calcium binding (Finn et al., 1995; Kuboniwa et al., 1995; Urbauer et al., 1995; Zhang et al., 1995). Calmodulin interacts with high affinity ($K_d \approx$ nM) with some 30 different proteins, and with numerous target peptide sequences derived from their calmodulin-binding regions. O'Neil and Degrado (1990) suggested that the propensity to form a basic amphipathic α-helix may be a common structural motif for many target sequences. Many of the known and putative target sequences have a bulky hydropho-

Reprint requests to: P.M. Bayley, Division of Physical Biochemistry, National Institute for Medical Research, The Ridgeway, Mill Hill, London NW7 1AA, England; e-mail p-bayley@nimr.mrc.ac.uk.

[1] Present address: Department of Chemistry and Biochemistry, Concordia University, 1455 de Maisonneuve Blvd. W., Montreal, Quebec H3G 1M8, Canada.

bic side chain near the N-terminus, usually flanked by one or more basic residues, and there is often a second bulky hydrophobic residue 13 residues later (Crivici & Ikura, 1995).

The structure of calmodulin complexed with M13, a 26-residue target peptide derived from the sequence of skeletal myosin light chain kinase (sk-MLCK), was determined from high-resolution NMR data by Ikura et al. (1992). The two domains of calmodulin surround the peptide, which adopts a mainly α-helical conformation, and the hydrophobic side chains of Trp-4 and Phe-17 of the peptide are exclusively involved in extensive hydrophobic contacts with the carboxy- and amino-terminal domains of CaM, respectively. Calmodulin–peptide complexes have been modeled extensively (Strynadka & James, 1990; Sekharudu & Sundaralingam, 1993). Recent crystal structures of complexes of calmodulin with target peptides from smooth muscle MLCK and CaM kinase II indicate a similar, though not identical, mode of interaction (Meador et al., 1992, 1993).

As noted by Ikura et al. (1992), the N-terminal peptide residues of the M13 target sequence interact predominantly with the C-domain of calmodulin and the C-terminal peptide residues with the N-domain of calmodulin. This suggests that the target sequence could be considered as comprising two smaller components. In previous work (Findlay et al., 1995a, 1995b), we used ^{1}H-NMR to identify the similarities in the interaction of calmodulin with two 18-residue peptides (WFF and FFW) and a 10-residue peptide (WF10), all based on the N-terminal sequence of M13, and showed that these peptides bind in similar orientation, with the N-terminal peptide residues interacting with calmodulin C-domain.

In this work, the interaction of calmodulin with two short peptides (WF10 and FW10, the first and last 10 residues of WFF and FFW, respectively) is examined. Both WF10 and FW10 have unprotected N- and C-termini. We compare the affinity and conformational properties of the complexes of these short peptides with calmodulin and TR2C (the calmodulin C-terminal domain) with those of the corresponding 18-residue sequences (WFF and FFW). We also study the mechanism of biphasic enhancement of calcium affinity of calmodulin by target sequences, and the mechanism of dissociation of WF10 from its complexes with Ca_4–CaM and Ca_2–TR2C using stopped-flow methods. In the presence of target peptides, the slow step of calcium dissociation (from the C-domain of calmodulin) proceeds from a partially saturated kinetic intermediate by a (reversible) relaxation mechanism. This mechanism is also found in the corresponding dissociation reactions of the full-length target sequences, and indicates that calmodulin dissociation from different targets can be discriminated by kinetic as well as equilibrium mechanisms (S.E. Brown, S.R. Martin, & P.M. Bayley, in prep.).

The results show that the target sequence of the sk-MLCK contains regions of different relative affinity for calmodulin. The interaction of the N-terminal half of the target sequence contributes the majority of the interaction energy, and causes selective enhancement of the affinity for two calcium ions in the calmodulin C-domain. The whole sequence (minimum 18 residues) is required for the induction of the full affinity for the target sequence and the full enhancement of affinity for four calcium ions, due to the cooperative interaction of the two contiguous elements of the target sequence with each of the calmodulin domains. However, the half-saturated complex suggests a novel mechanism of regulation of calmodulin–target interaction.

Results

Peptide affinities

The number of potential interactions between the N-terminal 18 residues of the M13 peptide (i.e., the WFF peptide) and residues in the N- and C-terminal domains of calmodulin as determined by NMR techniques (Ikura et al., 1992) is shown in Figure 1. The N-terminal region of the peptide interacts mainly with the C-domain of the calmodulin, and the C-terminal region of the peptide mainly with the N-domain of the protein.

The dissociation constants for the interaction of Ca_4–CaM and Ca_2–TR2C with the WFF and WF10 peptides are sufficiently low (<1 μM; see Table 1) to allow an accurate determination by direct fluorometric titration (data not shown, see Findlay et al., 1995b). The affinity of the WF10 peptide for intact calmodulin is effectively the same as that for the TR2C fragment, which is consistent with the view that the WF10 peptide interacts predominantly with the C-domain of calmodulin (Fig. 1). The possible interactions with the N-domain of the calmodulin (e.g., by I-9, A-10) are presumably not contributing significantly to the affinity. Increasing the length of the peptide to 18 residues (WFF peptide) increases its affinity for the TR2C fragment approximately 10-fold, indicating that, in the absence of the calmodulin, N-domain residues in the C-terminal half of the target sequence (e.g., Val-11) may contribute significantly to the interaction with the C-domain of calmodulin. The affinity of WFF for calmodulin is more than 400-fold higher than for the isolated C-domain, confirming the requirement for both domains of calmodulin to generate the very high affinity binding characteristic of target sequences.

The interaction of calmodulin with the FW10 peptide is considerably weaker and only an approximate dissociation constant could be measured. Figure 2A shows a direct fluorometric titra-

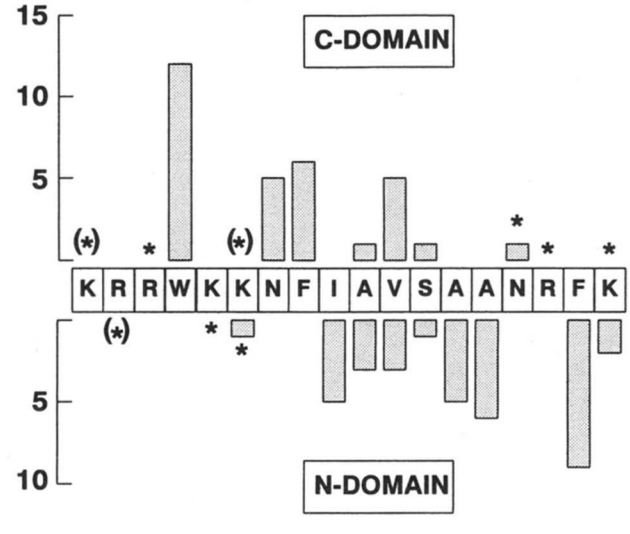

Fig. 1. Number of potential interactions between the N-terminal 18 residues of the M13 peptide (i.e., the WFF peptide) and residues in the N- and C-terminal domains of calmodulin. Electrostatic interactions are shown as *. Data are from the model of Ikura et al. (1992), deduced from NMR. Additional electrostatic interactions are indicated by (*), based on analogous residues in the X-ray crystal structure of CaM complexed with smooth muscle MLCK (Meador et al., 1992).

Table 1. *Dissociation constants for the interaction of calmodulin and TR2C with the WFF, WF10, and FW10 peptides (25 mM Tris, 100 mM KCl, 1 mM $CaCl_2$, pH 7.5, 30 °C)*[a]

Complex	K_d	$-\Delta G$ (kJ·mol^{-1})
Ca_4-CaM-WF10	735 (± 67) nM	35.6 (± 0.3)
Ca_2-TR2C-WF10	713 (± 115) nM	35.7 (± 0.5)
Ca_4-CaM-WFF	<0.2 nM[b]	>56.3
Ca_2-TR2C-WFF	76 (± 31) nM	41.3 (± 1.3)
Ca_4-CaM-FW10	85 (± 35) μM[c]	23.6 (± 1.3)
Ca_4-CaM-FW10	115 (± 40) μM[d]	22.9 (± 1.1)
Ca_2-TR2C-FW10	>100 μM	
Ca_4-CaM-FFW	1.6 (± 0.4) nM[b]	51.1 (± 0.6)

[a] All results are the average of at least three independent experiments (±SD).
[b] Value from Findlay et al. (1995b).
[c] Determined by fluorescence titration.
[d] Determined by near-UV CD titration.

tion of the FW10 peptide with calmodulin. The K_d determined from three titrations was 85 ± 35 μM. The ratio of the specific fluorescence of the complex to that of the free peptide was determined to be 2.4 ± 0.1 (cf. 3.0 for the 18-residue FFW peptide [Findlay et al., 1995b]). Figure 2B shows a near-UV CD titration of the calmodulin with the FW10 peptide. The K_d determined from three titrations was 115 ± 40 μM, in reasonable agreement with the value determined from the fluorescence titration. The molar CD extinction coefficients (at 278 nm) determined from the fit were -0.73 M^{-1}·cm^{-1} for Ca_4-CaM and -2.55 M^{-1}·cm^{-1} for the Ca_4-CaM-FW10 complex. The latter value is very close to that measured for the Ca_4-CaM-FFW complex (see below). The affinity of the FW10 peptide for calmodulin is ≈100-fold lower than that of WF10, indicating the importance of the interactions of the N-terminal region of the target sequence. The sum of the free energies for the interactions of the WF10 and FW10 peptides with calmodulin (-59.2 ± 1.6 kJ·mol^{-1}, see Table 1) may be compared with values of -56.3 kJ·mol^{-1} and -51.1 kJ·mol^{-1}, respectively, for the full-length WFF and FFW peptides.

Far-UV CD

A characteristic feature of the interaction of many target peptides with calmodulin is that the peptides adopt an α-helical conformation upon binding (O'Neil & Degrado, 1990). The number of residues in the peptide adopting a helical conformation in the complex was estimated as described in the Materials and methods. As shown in Table 2, even the 10-residue WF10 peptide adopts some helical structure upon interaction with either intact calmodulin or the TR2C fragment (≈3–4 residues). More α-helical structure is generated in the longer 18-residue WFF peptide upon binding to the TR2C fragment as a 1:1 complex (≈5–6 residues). The latter value should be compared with a value of ≈12–13 residues for binding of WFF to intact calmodulin (Findlay et al., 1995b). We note that these values are only approximate because they depend on the assumption that all the far-UV CD change can be attributed to increased helicity of the peptide. In fact, in NMR studies of the interaction of the M13 peptide with Ca_4-CaM, it was deduced that one turn of helical residues of calmodulin changed its conformation (Ikura et al., 1991).

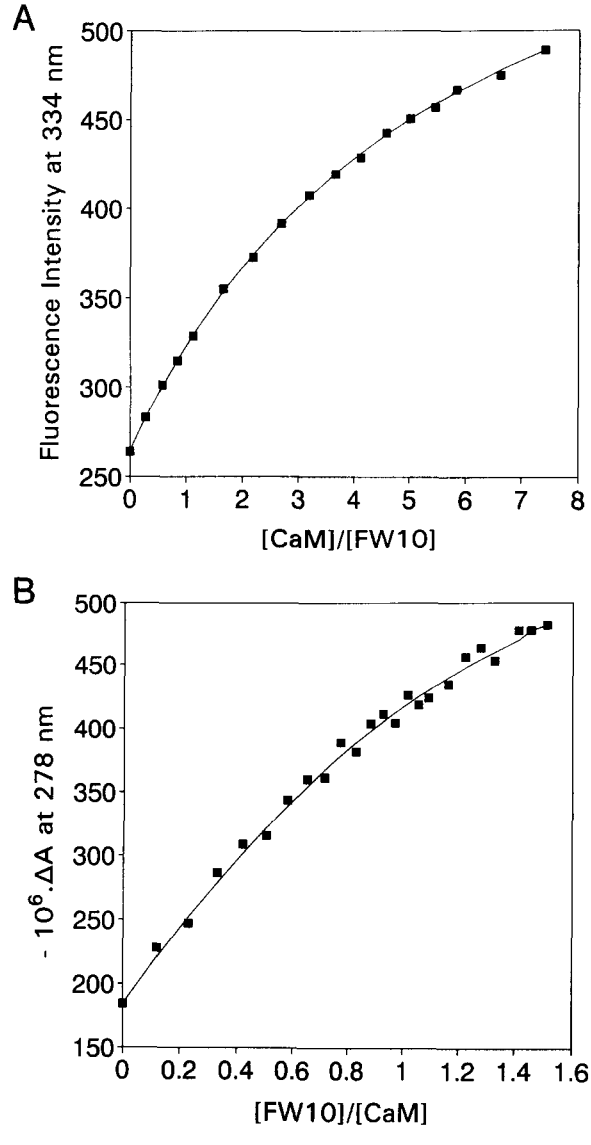

Fig. 2. Determination of the K_d for the interaction of the FW10 peptide with calmodulin. **A:** FW10 peptide (19 μM) was titrated with CaM and the fluorescence at 334 nm was recorded as a function of [CaM]/[FW10]. The solid line is the best fit to the data with a K_d of 79 μM. **B:** CaM (225 μM) was titrated with the FW10 peptide and the CD intensity at 278 nm was recorded as a function of [FW10]/[CaM]. The solid line is the best fit to the data with a K_d of 123 μM.

Near-UV CD

Figure 3A shows the near-UV CD spectra of Ca_4-CaM and its complexes with the WFF and WF10 peptides. The spectra of Ca_2-TR2C and its complexes with these two peptides are shown in Figure 3B. For both proteins, the spectrum of the complex with the WF10 peptide is significantly different from that with the WFF peptide. The difference spectra (calculated as {complex − components}; see Fig. 3C) for the two WFF complexes are closely similar, suggesting that the Trp-4 of the WFF

Table 2. *Molar CD extinction coefficients at 222 nm for TR2C and calmodulin alone, and for their complexes with the WF10 and WFF peptides*[a]

Protein or complex	$\Delta\epsilon_M$ (222 nm) (M^{-1} cm^{-1})[b]	$\Delta\Delta\epsilon_M$ (222 nm) (M^{-1} cm^{-1})[c]	N_H[d]
Ca_2-TR2C	−379	–	–
Ca_2-TR2C-WF10	−413	−34	3.8
Ca_2-TR2C-WFF	−432	−53	4.9
Ca_4-CaM	−771	–	–
Ca_4-CaM-WF10	−805	−34	3.8

[a] Spectra were recorded in 25 mM Tris, 100 mM KCl, pH 7.5, at room temperature.

[b] Molar CD extinction coefficient $\Delta\epsilon_M = \Delta\epsilon_{MRW} \times N_{res}$ (see the Materials and methods).

[c] $\Delta\Delta\epsilon_M$ was calculated as $\Delta\epsilon_M$ for the protein/peptide complex minus $\Delta\epsilon_M$ for the protein. The molar concentration of the protein/peptide complex was assumed to be equal to the total concentration of protein present.

[d] N_H is the total number of peptide bonds in the target peptide adopting an α-helical conformation on complex formation (see the Materials and methods).

peptide is bound in the same position in the complexes with the two proteins. Likewise, the difference spectra for the two WF10 complexes are also closely similar, suggesting that the Trp-4 in this peptide also binds in the same position in the complexes with the two proteins. However, the difference spectra for the WF10 complexes are very different from those calculated for the WFF complexes. This surprising observation suggests that the steric environment of the Trp-4 of the WF10 peptide complexed to Ca_4-CaM or Ca_2-TR2C is different from the Trp-4 in the corresponding complexes of the WFF peptide. The difference appears to be in a stronger negative ^{1}La transition for Trp-4 (in WF10), although both show a strong positive ^{1}Lb (fine structure) transition. In contrast, the spectra of the Ca_4-CaM-FFW and Ca_4-CaM-FW10 complexes are closely similar (Fig. 3D), suggesting that the position of the tryptophan in the complex is unaffected by removing the first eight residues of the FFW peptide. In this case, the CD is dominated by an even stronger negative ^{1}La transition, and the ^{1}Lb transition is almost unresolved.

Effect of target peptides on the affinity of calmodulin and TR2C for calcium: Stoichiometric calcium-binding constants

The indicator method (Linse et al., 1988, 1991a) has been used previously to determine the stoichiometric calcium-binding constants for calmodulin and its fragments. Here we extend the method to quantitate the observed increase in calcium affinity of calmodulin (and TR2C) in the presence of various dissociable target peptides; recently we have used a similar approach to measure the enhanced calcium affinity of a calmodulin-peptide hybrid protein (Martin et al., 1996). Typical experimental data for calcium titrations of 5,5′-Br_2BAPTA in the presence of CaM, CaM plus WF10 peptide, and CaM plus WFF peptide are shown in Figure 4A. The corresponding titrations for TR2C are shown in Figure 5A. The values of $\log(K_1 K_2)$ and $\log(K_3 K_4)$ determined for *Drosophila* CaM alone (see Table 3) agree reasonably well with values determined using the same technique with bovine testes CaM (Linse et al., 1991a) and with values determined using flow dialysis with cloned *Xenopus* CaM (Porumb, 1994). The values of K_1 and K_2 determined for TR1C and TR2C also agree reasonably well with those reported by Linse et al. (1991a).

For a four-site protein, the expressions that relate the stoichiometric Ca-binding constants ($K_1, \ldots, K_4$) to the site (or intrinsic) Ca-binding constants ($K_I, \ldots, K_{IV}$) for sites I and II (N-terminal domain) and III and IV (C-terminal domain) are extremely complex if one includes all potential interactions between the sites. Considerable simplification is possible if one pair of sites has substantially higher Ca affinity than the other. For example, if K_{III} and K_{IV} (C-terminal domain) are considerably stronger than K_I and K_{II} (N-terminal domain), then (Linse et al., 1991a):

$$K_1 \approx K_{III} + K_{IV},$$

$$K_2 \approx K_{III} \cdot K_{IV(III)}/(K_{III} + K_{IV}),$$

$$K_3 \approx K_{I(III\ \&\ IV)} + K_{II(III\ \&\ IV)},$$

$$K_4 \approx K_{I(III\ \&\ IV)} \cdot K_{II(I,\ III\ \&\ IV)}/(K_{I(III\ \&\ IV)} + K_{II(III\ \&\ IV)}),$$

where $K_{IV(III)}$ is the site binding constant for site IV when site III is already occupied, and so on. If there is no interaction between

Table 3. *Stoichiometric Ca^{2+} binding constants for CaM and TR2C in the presence and absence of WF10 and WFF peptides*[a]

Sample	n[b]	$\log(K_1)$	$\log(K_2)$	$\log(K_3)$	$\log(K_4)$	$\log(K_1 K_2)$	$\log(K_3 K_4)$
CaM	6	5.33 (0.14)	6.32 (0.20)	4.33 (0.31)	5.33 (0.20)	11.65 (0.08)	9.67 (0.19)
TR2C	5	5.32 (0.17)	6.21 (0.12)	–	–	11.53 (0.07)	–
TR1C	4	4.62 (0.13)	5.17 (0.14)	–	–	9.78 (0.09)	–
CaM: WFF	8	6.79 (0.23)	7.91 (0.25)	6.57 (0.24)	6.53 (0.21)	14.70 (0.16)	13.10 (0.17)
CaM: WF10	3	6.50 (0.14)	7.11 (0.27)	4.23 (0.30)	5.60 (0.27)	13.61 (0.12)	9.83 (0.17)
	3[c]	6.60 (0.16)	7.16 (0.17)	4.41 (0.27)	5.52 (0.27)	13.77 (0.09)	9.93 (0.05)
TR2C: WFF	3	6.15 (0.12)	7.35 (0.17)	–	–	13.50 (0.12)	–
TR2C: WF10	3	5.86 (0.08)	6.77 (0.21)	–	–	12.63 (0.14)	–

[a] Determined at 20 °C in 25 mM Tris, 100 mM KCl, pH 8.0.

[b] Number of titrations.

[c] Experiments performed at [WF10]/[CaM] ≈ 12.

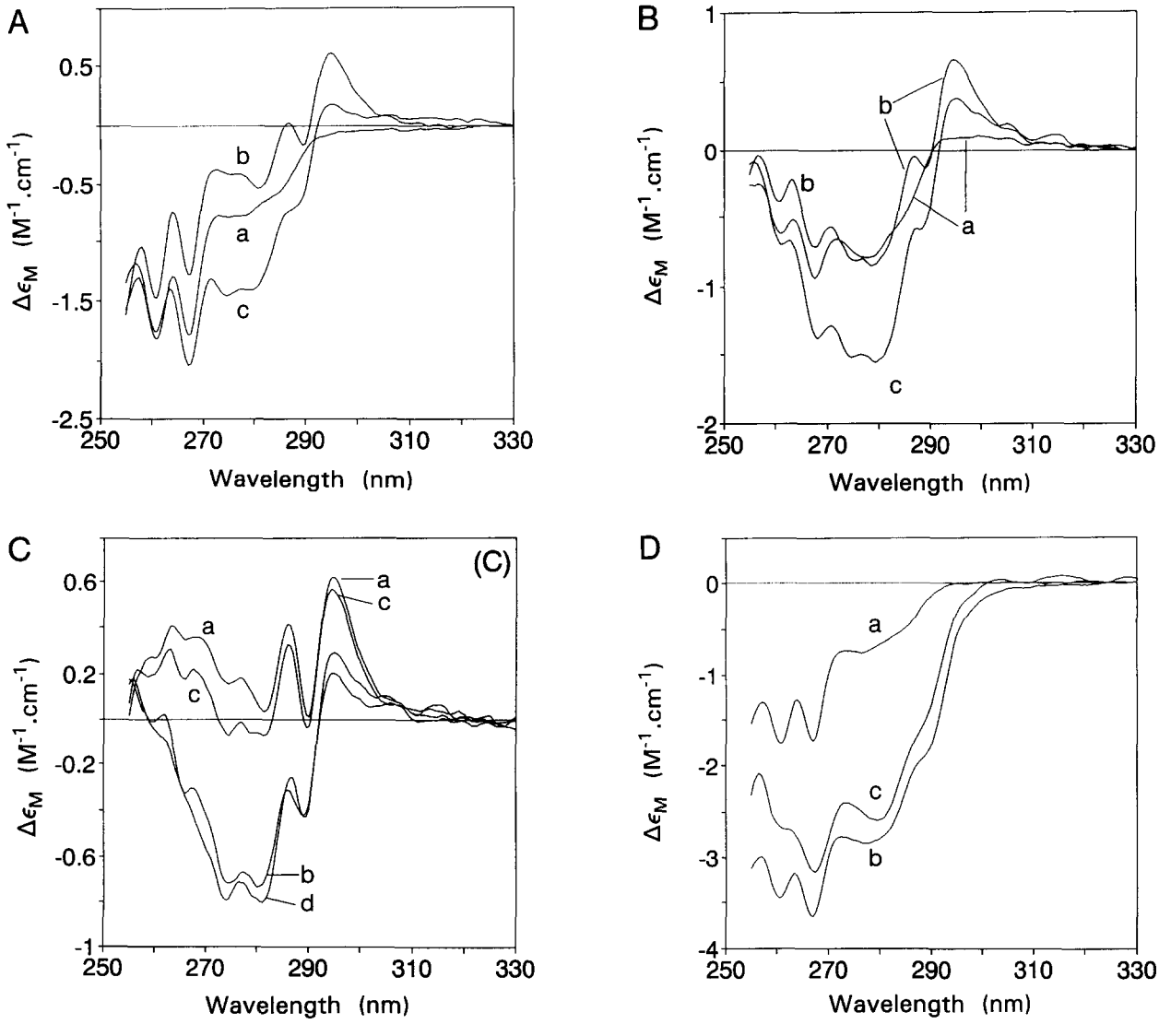

Fig. 3. A: Near-UV CD spectra of (a) Ca_4-CaM, (b) Ca_4-CaM-WFF, and (c) Ca_4-CaM-WF10. **B:** Near-UV CD spectra of (a) Ca_2-TR2C, (b) Ca_2-TR2C-WFF, and (c) Ca_2-TR2C-WF10. **C:** Difference spectra calculated as (complex − components) from the data of A and B. Spectra are for (a) Ca_4-CaM-WFF, (b) Ca_4-CaM-WF10, (c) Ca_2-TR2C-WFF, and (d) Ca_2-TR2C-WF10. **D:** Near-UV CD spectra of (a) Ca_4-CaM, (b) Ca_4-CaM-FFW, and (c) Ca_4-CaM-FW10. In the case of the FW10 peptide, the spectrum of the complex was derived from the experimental curves by assuming a K_d of $\approx$100 μM, the average of the values determined by fluorescence and near-UV CD titrations (see Table 1).

Ca-binding sites in *different* domains, then further simplification is possible as follows:

$$K_3 \approx K_I + K_{II},$$

$$K_4 \approx K_I \cdot K_{II(I)}/(K_I + K_{II}).$$

If this analysis is valid, then the values of K_1 and K_2 for whole CaM should be similar to the values of K_1 and K_2 for TR2C (which contains sites III and IV, only), whereas the values of K_3 and K_4 for whole CaM should be similar to the values of K_1 and K_2 for TR1C (which contains sites I and II, only). Inspection of the values reported in Table 3 for CaM and its tryptic fragments in the absence of added peptide show that this approach does indeed appear to be valid (cf. Linse et al., 1991a).

The stoichiometric Ca-binding constants given in Table 3 were used to calculate curves for the variation of the degree of saturation of CaM and TR2C with Ca as a function of $-\log([Ca]_{free})$. These are shown in Figure 4B (for whole CaM) and in Figure 5B (for TR2C).

Figure 4B shows that the affinity of all four Ca sites in CaM is increased dramatically in the presence of the WFF peptide (compare curves a and c). In contrast, the WF10 peptide (which lacks the eight C-terminal residues of WFF) produces a strongly biphasic Ca-binding profile (Fig. 4B, curve b), with occupancy by the third and fourth Ca ions being shifted only slightly from the curve for CaM alone. (A similar effect was observed for the interaction with the calmodulin C-domain of a part of the calmodulin-binding sequence from the plasma membrane calcium pump [Yazawa et al., 1992].) This suggests that binding of Ca

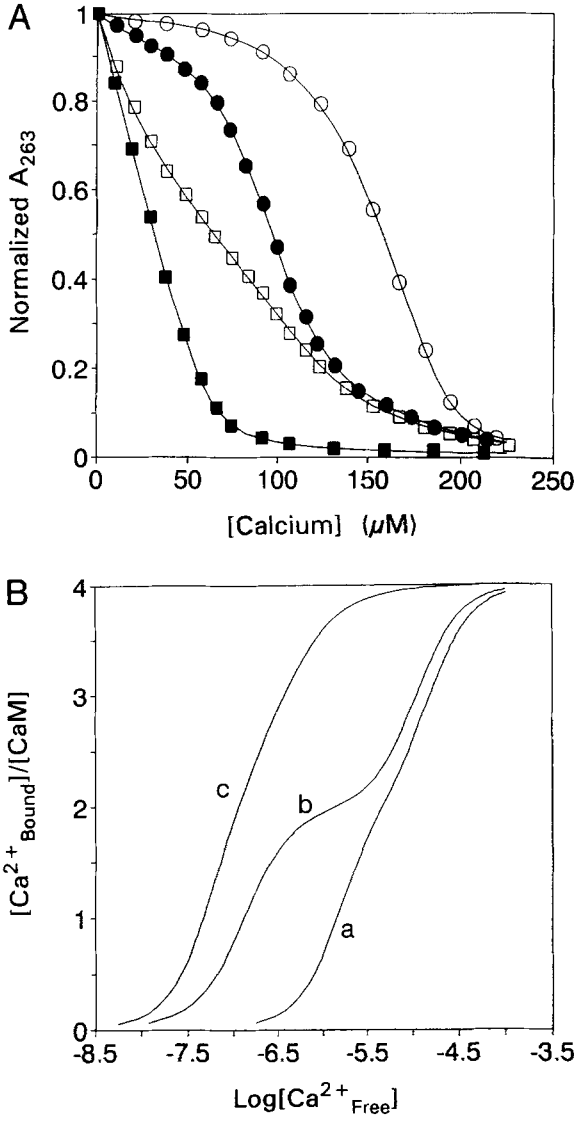

Fig. 4. A: Typical experimental data for calcium titrations of 5,5′-Br_2BAPTA (60.5 μM) in the absence of protein (■) and in the presence of 33 μM CaM (□), 33 μM CaM plus 146.8 μM WF10 peptide (●), and 33 μM CaM plus 119 μM WFF peptide (○). Curves through the points are the least-squares fits to the data. Total absorbance change has been normalized in order to facilitate comparison. **B:** Calcium binding to (a) CaM, (b) CaM in the presence of WF10 peptide, and (c) CaM in the presence of WFF peptide. Calcium-binding profiles were calculated from the stoichiometric binding constants determined from calcium titrations in the presence of 5,5′-Br_2BAPTA (CaM and CaM + WF10) or Quin 2 (CaM + WFF).

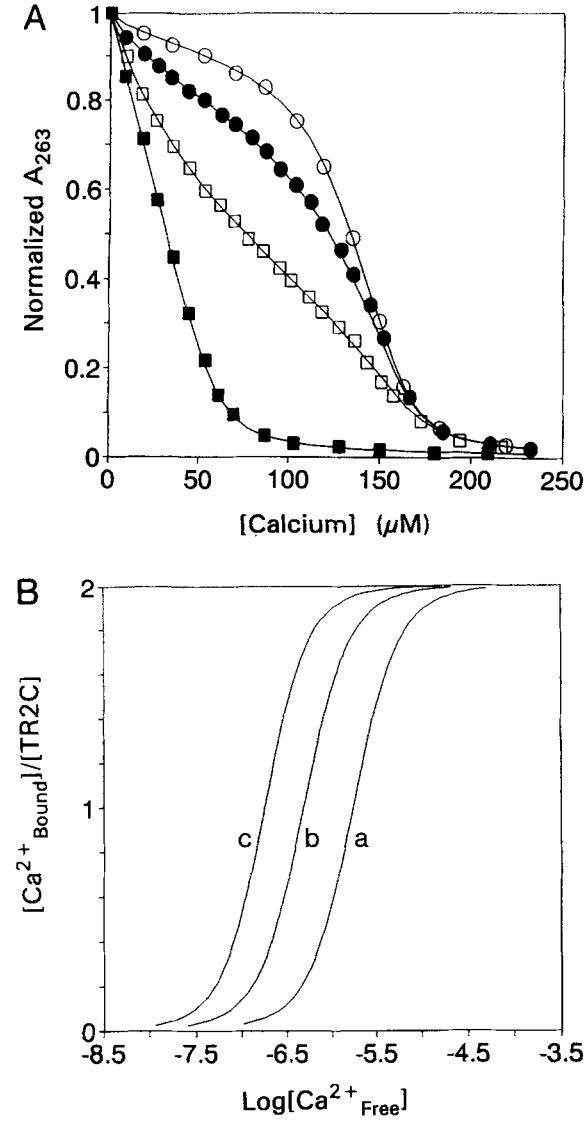

Fig. 5. A: Typical experimental data for calcium titrations of 5,5′-Br_2BAPTA (60.5 μM) in the absence of protein (■) and in the presence of 52.5 μM TR2C (□), 52.5 μM TR2C plus 125.3 μM WF10 peptide (●), and 52.5 μM TR2C plus 93.6 μM WFF peptide (○). Curves through the points are the least-squares fits to the data. Total absorbance change has been normalized in order to facilitate comparison. **B:** Calcium binding to (a) TR2C, (b) TR2C in the presence of WF10 peptide, and (c) TR2C in the presence of WFF peptide. Calcium-binding profiles were calculated from the stoichiometric binding constants determined from calcium titrations in the presence of 5,5′-Br_2BAPTA (TR2C and TR2C + WF10) or Quin 2 (TR2C + WFF).

to the C-terminal sites is enhanced significantly by the presence of the WF10 peptide, but that little enhancement of the Ca affinity of the N-terminal sites is seen. This is consistent with the view that the WF10 peptide forms contacts principally with the C-terminal domain of calmodulin, as deduced from the spectroscopic data reported here (see also Findlay et al., 1995a). However, the enhancement in the affinity of the C-terminal sites is considerably less for the WF10 peptide than for the WFF peptide. With TR2C, the Ca affinity (of sites III and IV) is also enhanced by the presence of peptide. The enhancement observed with WFF is considerably greater than that observed with WF10 (compare curves b and c in Fig. 5B). This is consistent with the observation that Ca_2-TR2C binds more strongly to WFF than to WF10 (see Table 1). The generally weaker interactions observed with WF10 and CaM (or TR2C) suggest that additional interactions can occur with the C-domain in the presence of the longer WFF peptide, or that the C-terminal negative charge of WF10 weakens the interactions.

For both WFF and WF10, the enhancement of the affinity of the C-terminal Ca sites is somewhat less for TR2C than it is

for intact CaM (see Table 3). For the WFF peptide, this presumably means that the C-terminal residues of the peptide make different contacts with the C-terminal residues of the CaM in the two cases. In the case of TR2C plus WFF peptide, it is not clear what contacts exist between the C-terminal portion of the peptide (normally interacting with the N-domain of CaM) and the TR2C. In the case of WF10, the explanation is less obvious because the affinity for the WF10 peptide is the same for the two proteins, which suggests that the interactions should be the same. There could, of course, be a difference in the affinity of this peptide for the apo form of the two proteins.

The Ca-induced increase in the affinity of CaM for a particular peptide may, in principle, be calculated from experimentally determined dissociation constants for the peptide in the presence (K_d) and absence (K'_d) of Ca. However, because the latter value is not generally accessible experimentally, an estimate of the ratio of the dissociation constants (K'_d/K_d) is frequently obtained from the measured stoichiometric Ca-binding constants determined for calmodulin alone ($K_1, \ldots, K_4$) and for calmodulin in the presence of excess peptide ($K'_1, \ldots, K'_4$) through equations such as (Yazawa et al., 1992):

$$K'_d/K_d = (K'_1 K'_2 K'_3 K'_4)/(K_1 K_2 K_3 K_4).$$

The K'_d/K_d values for a tryptic fragment of calmodulin may be calculated in a similar way (as $K'_d/K_d = (K'_1 K'_2)/(K_1 K_2)$). However, it should be noted that such calculations give only a *lower* limit for the ratio of the dissociation constants, because true values of K'_1-K'_4 will only be measured under conditions where the protein can be totally saturated with peptide in the *absence* of calcium. This is not generally achievable experimentally because the affinity of the peptide for the protein in the absence of Ca is generally low. Values of K'_d/K_d calculated from the data given in Table 3 are listed in Table 4.

Values for the Ca-induced enhancements of peptide affinity have been reported by Yazawa et al. (1992) for the binding of the calcium pump peptide C28W to calmodulin ($K'_d/K_d = 6.2 \times 10^8$) and to TR2C ($K_d/K'_d = 1.2 \times 10^3$). The enhancement calculated for WFF binding to intact CaM is much greater than that calculated for the binding of WF10 to CaM or for the binding of WF10/WFF to TR2C. This confirms that the binding of Ca to the N-terminal sites of CaM makes a major contribution to the overall Ca-induced increase in peptide affinity.

Table 4. *Ca^{2+}-induced enhancement of peptide affinities for CaM and TR2C interacting with WF10 and WFF peptides calculated from the stoichiometric binding constants given in Table 3*

Protein	Peptide	K_d (nM)	K'_d/K_d[a]	K'_d (M)[b]
CaM	WFF	<0.2	3.1 (± 1.2) × 10^6	<6.2 × 10^{-4}
	WF10	735	270 (± 140)	2.0 × 10^{-4}
			830 (± 280)[c]	6.0 × 10^{-4}
TR2C	WFF	76	150 (± 50)	11 × 10^{-6}
	WF10	713	22 (± 10)	16 × 10^{-6}

[a] Calculated from the stoichiometric calcium-binding constants measured in the presence and absence of peptide as described in the text. K'_d and K_d are the dissociation constants for peptide binding to calmodulin in the absence and presence of calcium. Note that this ratio is a lower estimate for the relative affinity of peptide for Ca_4-CaM versus apo-CaM (or Ca_2-TR2C versus apo-TR2C; see text).

[b] Calculated using the measured K_d values.

[c] Calculated from the stoichiometric Ca^{2+} binding constants measured at a [WF10]:[CaM] ratio of 12:1.

Taken at face value, the results in Table 4 suggest that peptide affinities in the absence of Ca range from ≈0.6 mM (for CaM:WFF) to 16 μM (for TR2C:WF10). These are *lower* limits (owing to the uncertainties inherent in the determination of $K'_1, \ldots, K'_4$, as noted above), but the results do suggest that all peptides bind with similar affinities in the absence of Ca. Affinities in this range have been reported for the interaction of other peptides with CaM in the absence of Ca (Olwin & Storm, 1985; Yazawa et al., 1992).

Stopped-flow kinetics of calmodulin-WF10 and TR2C-WF10 complexes

We have used stopped-flow techniques to study the dissociation of the Ca_4-CaM-WF10 and Ca_2-TR2C-WF10 complexes. Dissociation was induced by the addition of Quin 2 or EGTA and monitored by Quin 2 or peptide tryptophan fluorescence. The results for dissociation of Ca_2-TR2C and the Ca_2-TR2C-WF10 complex are shown in Figure 6A. In the absence of added peptide, the dissociation rate monitored by Quin 2 fluorescence is monophasic (k_{obs} = 16.4 s^{-1}), confirming that the two calcium ions dissociate with identical rates or that slow dissociation of one calcium is followed by rapid loss of the other. Dissociation of the Ca_2-TR2C-WF10 complex (at [WF10]/[TR2C] = 1) is also monophasic, but is slower by a factor of almost two (k_{obs} = 8.1-9.6 s^{-1}). At higher peptide to protein ratios, the observed dissociation rate is significantly slower (≈5.3 s^{-1} at [peptide]/[TR2C] = 2 and 3.5 s^{-1} at [peptide]/[TR2C] = 4:1). The rates measured using the two probes (Quin 2 fluorescence or EGTA with peptide tryptophan fluorescence) are very similar, although the rates measured using Quin 2 are somewhat faster, especially at low peptide to protein ratios.

Results for dissociation of the Ca_4-CaM-WF10 complex are shown in Figure 6B. For calmodulin alone, a single dissociation step is observed in the Quin 2 experiments with $k_{obs} \approx 15$ s^{-1}; this agrees reasonably well with a previous value of 11 s^{-1} at 18 °C measured for dissociation of calcium from the C-domain sites (Martin et al., 1992) and is very similar to the value measured for TR2C alone (see above). Dissociation of calcium from the N-domain sites (>800 s^{-1}, Martin et al., 1992) is expected to be too fast to be observed in these experiments because most of the reaction amplitude would be lost in the instrument deadtime. Formation of the 1:1 complex with WF10 again reduces the dissociation rate, which, as in the case of TR2C, is slower at higher peptide to protein ratios (see Fig. 6B). As in the case of the TR2C complex, the dissociation rates observed using Quin 2 are somewhat faster than those observed using peptide tryptophan fluorescence. Overall, the rates observed with intact calmodulin are very similar to those observed with TR2C. The kinetics of dissociation of the Ca_4-CaM-WFF complex are more intricate, showing biphasic kinetics, and will be discussed in detail elsewhere (S.E. Brown, S.R. Martin, & P.M. Bayley, in prep.).

We attempted to measure association rate constants by mixing 1 μM WF10 with 10 μM TR2C or calmodulin in buffers containing 1 mM $CaCl_2$. Under these conditions, the reaction was

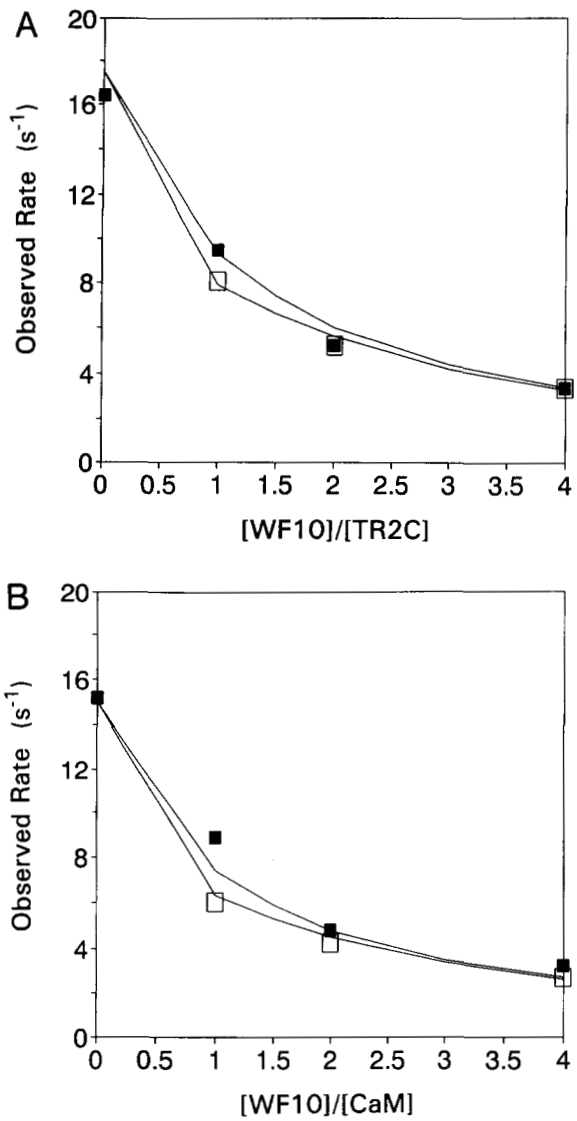

Fig. 6. Stopped-flow kinetics of dissociation of protein-peptide complexes following the addition of an excess of a calcium chelator, Quin 2, or EGTA. **A:** Observed rates of dissociation for the Ca_2-TR2C-WF10 complex monitored using Quin 2 fluorescence (■) and peptide tryptophan fluorescence (□). The solid lines are computer simulations of path A in Figure 7 using $k_1 = 1.0 \times 10^9\ M^{-1} \cdot s^{-1}$, $k_{-1} = 750\ s^{-1}$, and $k_{-2} = 17.5\ s^{-1}$. The upper line is the simulation for Quin 2 fluorescence, the lower line is that for peptide tryptophan fluorescence. **B:** Observed rates of dissociation for the Ca_4-CaM-WF10 complex monitored using Quin 2 fluorescence (■) and peptide tryptophan fluorescence (□). The solid lines are computer simulations of path A in Figure 7 using $k_1 = 1.0 \times 10^9\ M^{-1} \cdot s^{-1}$, $k_{-1} = 750\ s^{-1}$, and $k_{-2} = 15\ s^{-1}$. The upper line is the simulation for Quin 2 fluorescence, the lower line is that for peptide tryptophan fluorescence.

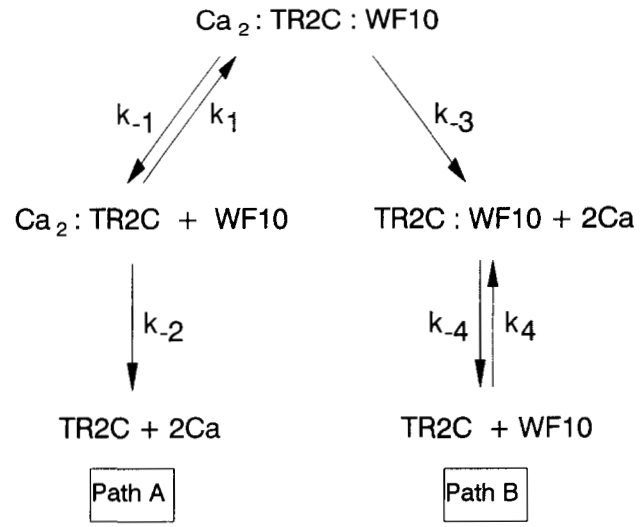

Fig. 7. Kinetic scheme for the dissociation of the Ca_2-TR2C-WF10 complex following the addition of an excess of a calcium chelator (Quin 2 or EGTA). The steps involving calcium dissociation are irreversible because the chelator is added in large excess.

at least 95% complete within the deadtime of the instrument, suggesting that the association rate constant, k_{on}, is greater than $5.0 \times 10^8\ M^{-1} \cdot s^{-1}$.

Two possible pathways for the Quin 2- or EGTA-induced dissociation of the Ca_2-TR2C-WF10 complex are shown in Figure 7. In path B, the calcium ions are lost from the Ca_2-TR2C-WF10 complex in step 3. The peptide then dissociates from the apoprotein to which it is only weakly bound (step 4). If step 4 is fast, as seem likely, then step 3 will be rate limiting for both signals (tryptophan and Quin 2). The observed rate of dissociation will not then depend upon the peptide to protein ratio. Even if the peptide release step (step 4) was slow, the observed rate measured with Quin 2 would remain independent of the peptide to protein ratio. In a recent study with full-length sk-MLCK peptides (S.E. Brown, S.R. Martin, & P.M. Bayley, in prep.), we have shown that an alternative pathway must be considered (path A in Fig. 7). Under the conditions of the stopped-flow experiments, the Ca_2-TR2C-WF10 complex is in rapid equilibrium with Ca_2-TR2C and free peptide. Following dissociation of the peptide in step 1, the peptide can rebind (with bimolecular rate constant k_1) or the calcium ions can dissociate (step 2) with rate constant k_{-2} ($\approx 16.4\ s^{-1}$, see Fig. 6A). The competition between peptide rebinding (k_1) and calcium loss (k_{-2}) will reduce the observed rate constant for calcium appearance to less than $16.4\ s^{-1}$. At higher peptide to protein ratios, the rebinding will compete more effectively with calcium loss and the observed rate will be reduced still further. Computer simulations with the parameters given in the legend to Figure 7 show that path A can indeed reproduce the observed experimental behavior. The observation that the rate observed with Quin 2 is faster than that observed with peptide tryptophan fluorescence (particularly at low peptide to protein ratios) is also reproduced in the simulations. This effect derives from the fact that not all of the TR2C is complexed to peptide under the conditions of the stopped-flow experiment. This, in turn, means that, in the Quin 2 experiments (but not in the tryptophan fluorescence experiments), one observes convolution of path A with direct dissociation from the small amount of uncomplexed Ca_2-TR2C. The behavior observed with Ca_4-CaM-WF10 is also reproduced in computer simulations (see Fig. 6B). Under the conditions employed, the dissociation of Ca from the N-terminal sites of calmodulin (which we assume is unaffected by the presence of the WF10 peptide) is too fast to be seen. It should be noted that the stopped-flow experiments give no information about the

value of the rate constant for dissociation of calcium from the Ca_2–TR2C–WF10 or Ca_4–CaM–WF10 complexes. This analysis of the results shows the formation of an intermediate species of calmodulin–peptide complex with half saturation of the calcium sites (i.e., Ca_2–CaM–peptide) and the potential role of such an intermediate in determining the rate of dissociation of the CaM–peptide complex.

Discussion

Experimental dissection of the target sequence

Understanding of the detailed mechanism of the interaction of calmodulin with its target enzymes is complicated by the diversity of sequences of the calmodulin binding regions of these proteins. Crivici and Ikura (1995) have provided a rationalization of many of these sequences in terms of the generality of certain structural features, including: (1) the adoption of predominantly α-helical conformation on binding to calmodulin and (2) the existence of two bulky hydrophobic residues separated by 12 other residues (Ikura et al., 1992, the $Bx_{12}B$ motif). In the case of the M13 peptide sequence, these residues are Trp-4 and Phe-17. Our studies with variants of the M13 sequence have a direct bearing on this hypothesis.

The series of peptides with different permutations of residues at positions 4, 8, and 17 (WFF, FWF, FFW, and FFF) all have high affinity for CaM, with K_d, respectively, <0.2 nM, 6.2 nM, 1.6 nM, and 0.8 nM (Findlay et al., 1995b; S.R. Martin, unpubl.), suggesting a general conformity with this motif. It was shown by NMR that WFF, FFW, and WF10 all bind to calmodulin in the same mode, hence possible reversal of peptide orientation is excluded (Findlay et al., 1995a). The present work supports this concept: the shorter peptide WF10 binds to CaM and to TR2C with effectively identical CD properties of residue Trp-4, which must interact with the C-domain. On binding to CaM, the CD spectra of peptides FFW and FW10 (residues 9–18 of FFW) are similar to each other, but distinctly different from the spectra of bound WF10. This shows that residue Trp-17 interacts with the N-domain. In all complexes of CaM with these tryptophan-containing peptides, the fluorescence emission is characteristic of tryptophan in a buried hydrophobic environment.

These results qualitatively support the key role of bulky hydrophobic residues in positions 4 and 17, and suggest the possibility of subdividing the target sequence into smaller entities to examine the component interactions. In fact, the affinities of the shorter peptides WF10 and FW10 show marked differences, with K_d 0.7 μM and 100 μM, respectively. This difference may reflect the presence of the N-terminal basic residues in WF10 that are absent from FW10, but may also suggest that the hydrophobic interaction of residue Trp-4 with the C-domain is stronger than that of residue Trp-17 with the N-domain. In this context, it is interesting that other target sequences for which structural data are available show stronger identity at the Trp-4 residue, whereas residue 17 is replaced (conservatively) by residue Leu-17 in sm-MLCK, and, in CaM–KII, it is Leu-13 that interacts with the N-domain (Meador et al., 1992, 1993). In principle, it should be possible to compare the total free energy of interaction of the partial sequences with that of the full WFF (or FFW) sequence: this might be expected to show a significantly stronger interaction for the full sequence, owing to the favorable steric or entropic effect of presenting the single contiguous sequence to the binding site. In practice, such comparison becomes difficult when the highest affinities are at the limit of measurement (as here), and would also depend on precise additivity of the peptide sequences, allowance for charged end effects, and the demonstration that the atomic details of binding are identical for both the full sequence and the subsequences. Given the unstructured nature of the free peptides, and the potential relative mobility of intact calmodulin itself, such criteria cannot be realistically met in the present case. It is, however, interesting that Persechini et al. (1994) were able to rationalize the greater affinity of whole calmodulin for sk-MLCK enzyme compared to the sum of the affinities for the two separate domains, a situation with some formal similarity to the present case.

The kinetic properties of the complex between calmodulin and WF10 are illuminating in two respects: first, in view of the observed decrease of peptide dissociation rate with increasing peptide concentration (Fig. 6), it is possible to assign the slowest step in the dissociation of the peptide complex on removal of calcium to a reversible peptide dissociation from a half-saturated intermediate species, Ca_2–CaM–WF10, rather than direct Ca ion dissociation; second, the presence of this intermediate (which is analogous to a similar half-saturated kinetic intermediate formed on dissociation of Ca in the presence of the full WFF sequence) shows that an intermediate state of Ca dissociation can exist on the kinetic time scale. This intermediate could be a point at which further kinetic regulation could be introduced, by virtue of differences in the target sequences, and hence could contribute to the diversity of properties required to allow kinetic discrimination in the interaction of calmodulin with different targets.

The role of individual domains in calmodulin–target interactions

Extensive previous work has considered the role of individual calmodulin domains to activate a target enzyme (see Klee, 1988 for review). In general, isolated calmodulin domains show low efficiency as activators either in isolation or in combination, (Newton et al., 1984). An exception is seen with the activation of the erythrocyte Ca pump by the TR2C domain (Guerini et al., 1984), consistent with the unusual sensitivity of the activation of this enzyme to mutation of Ca sites in the C-domain of calmodulin (Gao et al., 1993). In recent work by Persechini et al. (1994), it is shown that sk-MLCK, sm-MLCK, and neuronal nitric oxide synthase (NOS) can be activated to 65–80% maximal activity by the simultaneous binding of isolated C- and N-domains of calmodulin, and it is deduced that calmodulin itself binds in an ordered mechanism with the C-domain binding with higher affinity. Efficient activation apparently requires both domains of calmodulin to interact with the target sequence. Thus, one may ask whether the two domains have a single integrated role or whether they possess distinctive functions?

A key observation is the enhancement of calcium affinity by peptide binding to calmodulin (Maulet & Cox, 1983; Olwin & Storm, 1985; Yazawa et al., 1987, 1992). This follows naturally from the linked thermodynamics of calcium and peptide binding. However, this effect may present a problem for the control of calmodulin–target interactions by purely associative mechanisms, because the calmodulin target complex is now signifi-

cantly stabilized. As can be seen from Figure 4B, the [Ca] must be reduced to pCa > 8 to dissociate the calmodulin-target peptide complex into its components. However, the demonstration of the biphasic calcium saturation curve for the complex of CaM with WF10 suggests another, more general mechanism for the calmodulin-dependent regulation of enzyme activation by changes in the cytoplasmic calcium ion concentration. The plateau of the biphasic curve in Figure 4B indicates the existence, as a stable equilibrium species, of the complex Ca_2-CaM-peptide, which would exist at pCa ≈ 6 (see Fig. 4B). Dissociation of the target sequence would only occur if the Ca concentration is reduced to pCa ≈ 8. It may be noted (Table 3) that the enhancement of C-domain Ca affinity by WF10 is dependent upon the peptide concentration. (Simulation shows that this is a general effect such that the enhancement increases at higher peptide concentration [S.R. Martin, unpubl.].) The question thus arises of the nature of the species present as a function of [Ca] for the full peptide WFF in the presence of CaM. We have shown (Martin et al., 1996) by titration of apo-CaM with Ca in the presence of WFF that the change in tryptophan fluorescence is 75–80% complete at 2 Ca/CaM. This shows that the preferential interaction is between the C-domain and the N-terminal sequence of WFF. The intrinsic higher affinity for Ca of the C-domain of CaM alone compared to N-domain is seen in Table 3 (for CaM itself, $K_1K_2 > K_3K_4$, and for the separate domains, K_1K_2 (TR2C) > K_1K_2 (TR1C)). This relationship is preserved in the presence of the target peptide WFF. Thus, the complex present at 2 Ca/CaM in the presence of WFF must be (predominantly) Ca_2-CaM-peptide, with two Ca at the C-domain sites, and the calmodulin N-domain no longer interacting with the target sequence. This may be contrasted with the behavior of the calmodulin-peptide hybrid protein (containing the M13 sequence covalently attached to the C-terminus of calmodulin). In this case, the formation of the complex is highly cooperative, and the binding of four Ca ions is required to achieve saturation of binding by the attached peptide sequence (Martin et al., 1996). Thus, the intrinsic differences in the two domains of calmodulin—which are strongly conserved in evolution across a wide range of calmodulins—may be essential to allow a specific role to both domains in the process of target recognition.

Assuming these considerations can be applied to the interaction of calmodulin with the target enzyme, reversal of the activation by calmodulin would require [Ca] to be lowered only to pCa ≈ 7, when the N-domain would no longer interact, rather than to pCa > 8 to cause full dissociation of the complex. This mechanism would also imply that calmodulin could remain attached to the target, via the C-domain, although the system would not be activated: it is interesting that a recent study has shown that ≈ 95% of calmodulin in smooth muscle cells is apparently not free to diffuse, even when the system is deactivated at low [Ca], (Luby-Phelps et al., 1995). By contrast, calmodulin in unstimulated fibroblasts is reported to be largely diffusible (Gough & Taylor, 1993).

Hypothesis: A general mechanism for calmodulin-target interactions

These results suggest a general mechanism for enzyme regulation by calmodulin for the normal case where activation requires both domains of calmodulin to be bound. This mechanism is based on the observed differential affinity of the interactions of N- and C-domains with the target sequence, which is equivalent to a differential sensitivity of the two interactions for Ca ion concentration. This naturally leads to the possibility of the existence of an intermediate inactive calmodulin-enzyme complex at resting [Ca] in the range from 10^{-8} to 10^{-6} M. This is shown in Figure 8 based on the intrasteric and pseudosubstrate inhibition mechanism reviewed in Crivici and Ikura (1995). The activated state (State III) occurs at highest [Ca] and is depicted as requiring the binding of both domains of calmodulin to target sequences in the species Ca_4-CaM-enzyme: in this state, the regulatory domain is detached from the catalytic domain, which is fully activated. If the calmodulin C-domain binds more strongly than the N-domain, then as [Ca] is progressively lowered, an intermediate state (State II) will be reached in which the complex has the form Ca_2-CaM-enzyme, with two Ca in the C-domain; the N-domain is no longer bound or effective, and the regulatory domain binds to the catalytic domain so that the complex is inactive. Full dissociation of calmodulin would require the prevailing [Ca] to be lowered to extreme values—a process that could require expenditure of considerable amounts of metabolic energy—producing the dissociable apo-CaM and the inactive enzyme (State I).

This general mechanism has the advantage that calmodulin would still act in a Ca-dependent manner; dissociation of the calmodulin would not be obligatory, but could be controlled by the appropriate cytoplasmic Ca concentration to maintain the interaction of the C-domain with the given target sequence. Such a mechanism could also include protein modification to reduce the interaction of one calmodulin domain with its portion of the target sequence, for example, by phosphorylation of the target or calmodulin itself (see Crivici & Ikura, 1995 for a review). Activation of the intermediate complex by Ca would be prompt and efficient, because priority would be given to enzymes that already were in the Ca_2-CaM-enzyme intermediate state. It would be rapid because it would only require binding of additional Ca at the (kinetically fast) N-domain sites, and would avoid the necessity for diffusion of Ca_4-CaM formed at distant cytoplasmic locations. Such a mechanism would allow rapid response to transient increases of Ca—such as required in skeletal muscle contraction and response to cytoplasmic Ca waves. For other calmodulin-dependent processes that do not require a fast time response, a calmodulin target complex would be preferred in which the affinities of the C-domain and N-domain for the target were more nearly equal; binding of Ca_4-CaM and enzyme activation would be more directly coupled, and would follow the formation of the Ca_4-CaM species in the cytoplasm via a direct pathway between States I and III.

This hypothesis suggests a possible differential role for the two domains of calmodulin. The C-domain shows the higher affinity for its portion of the target sequence, and is postulated to be responsible for calmodulin binding in the absence of enzyme activation. Binding of Ca at the N-domain is postulated to provide the rapid response in transition from inactive Ca_2-CaM-enzyme to Ca_4-CaM-enzyme, during which it should become specifically bound to the enzyme. The mechanism would apply equally to calmodulin binding in a more "closed" conformation to a more contiguous target sequence (cf. the calmodulin complex with CaM-kinase II [Meador et al., 1993]), or in a more "open" conformation to a discontinuous pair of target sequences. Also, the model is based on the data for the sk-MLCK

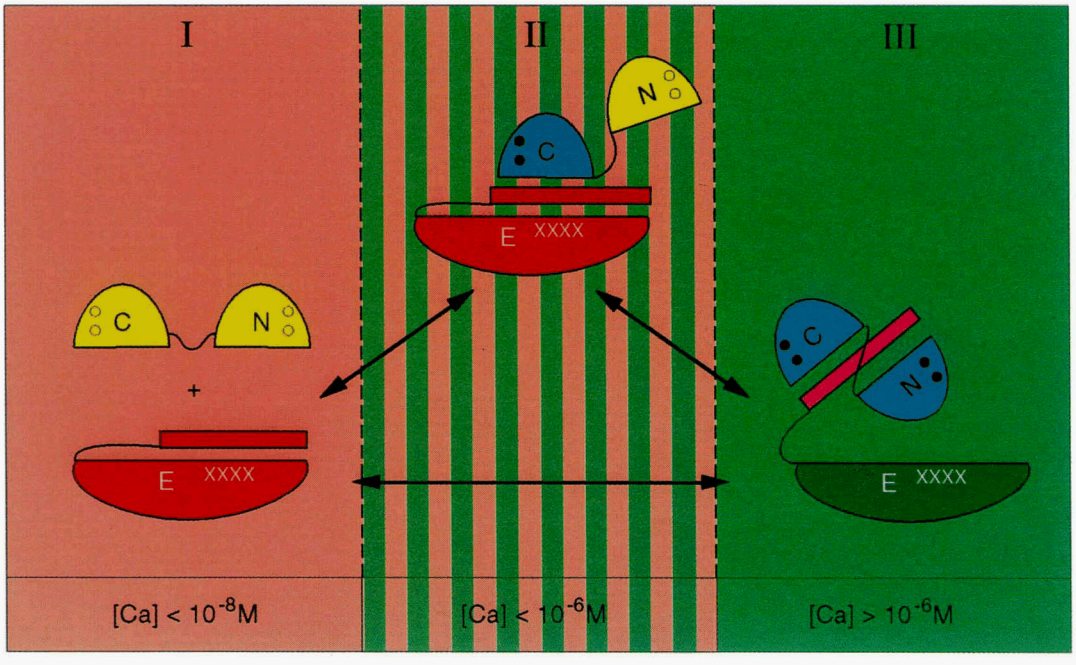

Fig. 8. General mechanism for calmodulin–target enzyme interactions based on CaM–skMLCK peptide interactions. The enzyme E contains a catalytic domain (large) and a regulatory domain (small) comprising pseudosubstrate and calmodulin-binding sequences: calmodulin is shown schematically as two domains, N and C, joined by a flexible tether; apo-calmodulin is shown yellow and calcium binding indicated by filled circles. At the lowest [Ca], the regulatory domain inhibits the active site (xxxx) and *State I is inactive* (red). At [Ca] from 10^{-8} M to 10^{-6} M, the intermediate complex Ca_2–CaM–enzyme is formed, with two Ca bound in the C-domain (blue). The regulatory domain remains in place and *State II is also inactive* (red). At the highest [Ca] the calmodulin becomes fully saturated (blue), both calmodulin domains bind to the regulatory domain (magenta), giving the complex Ca_4–CaM–enzyme, and the inhibitory regulatory domain is displaced, freeing access to the active site. *State III is fully activated* (green). Activation can occur directly between States I and III, or from the intermediate State II to State III, depending on the relative affinities of the C- and N-domains of calmodulin for the target sequence, and the resting calcium ion concentration.

peptides, and is drawn to illustrate the greater affinity of the C-domain of CaM for the target sequence, reflecting its greater affinity for the Ca ion. However, the reverse situation is, in principle, possible for a different target sequence, if the Ca-dependent binding of the N-domain would be stronger. Likewise, dependent on the target sequence, complex formation could in general involve alternative orientations and different positions of the two domains relative to the polarity of the target sequence. The crucial factor is the differential Ca-dependent affinity of the two parts of the calmodulin structure for the target.

The main feature of this mechanism is that the intermediate species functions to uncouple the initial step of calmodulin binding from subsequent enzyme activation, so that these processes can occur at different levels of cytoplasmic [Ca]. The experimental test of this requires direct measurement of the affinity of isolated C- and N-domains with target enzymes. In general, there is relatively little information currently available. However, the studies of Persechini et al. (1994) provide lower estimates for such affinities, based on enzyme activation assays. These authors identified two sites (A and B) as the principal binding sites for C-domain and N-domain, respectively. For the sk-MLCK, site A may be identified as the N-terminal portion of the target sequence (i.e., the part of M13 corresponding to the WF10 sequence), and similarly for sm-MLCK and NOS. The apparent K_d values for TR2C (site A) are 0.3 μM, 1.2 μM, and 10 nM for these three enzymes, respectively, but, because these derive from competition against 3–10 nM calmodulin, the values could be significantly lower. Most important, these data demonstrate that (for sk-MLCK and sm-MLCK) site A binding of TR2C competes against calmodulin and restores the inhibited state. This fits well with the properties expected for the analogue of State II of Figure 8, namely, Ca_2–TR2C–enzyme, where the C-domain has bound to the enzyme, but has not activated it. TR1C likewise can compete with calmodulin to give an inhibited state. The apparent affinity for TR1C is generally less than that for TR2C, which is again consistent with the formulation of the general mechanism of Figure 8.

In addition, several of the postulates of the model are amenable to experimental testing. For example, (1) the activation step (State II to State III) is centered on the binding of the N-domain so that a peptide specific for the N-domain should inhibit activation without necessarily causing dissociation of calmodulin; (2) competition between target peptides with calmodulin may be expected to be kinetically complex; (3) fast and slow calmodulin-dependent activations may have different characteristics in the target sequences of the enzymes involved; and (4) weaker binding targets should activate at higher [Ca] concentrations. These questions are presently under investigation.

Since submission of this work, we note the appearance of two relevant kinetic papers. Persechini et al. (1996) show that inactivation of Ca-CaM-dependent NOS by EGTA is faster than the slowest step of calcium dissociation, indicating the presence of

a deactivated intermediate species; by contrast, inactivation and dissociation by EGTA of the activated sk-MLCK followed similar kinetics. Johnson et al. (1996) also noted the biphasic nature of Ca dissociation from CaM–peptide complexes by chelators, indicative of intermediate species, and likened the intermediate state to that of the inactive state of the troponin complex of skeletal muscle, when Ca has dissociated from the N-domain sites of troponin C.

Conclusion

We therefore conclude that the existence of intermediate species in the interaction of calmodulin and the WFF sequence of M13 has potential structural and mechanistic significance. The use of the peptide WF10 provides a model for the intermediate species in the interaction of CaM with peptide M13, which is most obviously implied by both the structural and kinetic results. Calmodulin interacts with a diverse range of target sequences with only limited identity or homology between them. We suggest that the differences of sequence may have an important function, and be an essential requirement to provide the range of affinities and rates of partial reactions necessary to satisfy the diversity of calmodulin-dependent functions. The present results show how an individual target sequence can be subdivided or dissected into shorter sequences, which indicates the distinctive role of small numbers of residues in determining the characteristic domain interactions of a given calmodulin–target complex. The existence of intermediate species also suggests general principles for calmodulin target interactions involving a differential role for the two domains. This allows the diversity of target sequences to be translated into different activation properties with a range of calcium sensitivities and temporal responses.

Materials and methods

Proteins and peptides

Drosophila melanogaster calmodulin expressed in *Escherichia coli* was purified as described in Findlay et al. (1995b). The N- and C-terminal tryptic fragments of bovine calmodulin (TR1C and TR2C) were kindly provided by Prof Sture Forsén (University of Lund, Sweden). The peptides WFF (KKRWKKNFIA VSAANRFK), WF10 (KKRWKKNFIA), FFW (KKRFKKNF IAVSAANRWK), and FW10 (IAVSAANRWK) were synthesized on an Applied Biosystems 430A peptide synthesizer. They were purified by HPLC on a C18 column and were provided with free carboxy and amino termini. All concentrations were determined spectrophotometrically using an extinction coefficient of 5,560 M^{-1} cm^{-1} at 280 nm for the peptides (calculated for 1 tryptophan, Gill & von Hippel, 1989) and published extinction coefficients of 2,120 $M^{-1}\cdot cm^{-1}$ at 259 nm or 1,578 $M^{-1}\cdot cm^{-1}$ at 279 nm for intact *Drosophila* calmodulin in the presence of calcium (Maune et al., 1992b) and 3,300 $M^{-1}cm^{-1}$ at 277 nm for bovine TR2C in the presence of calcium (Klee, 1977).

Determination of peptide affinities

Peptide affinities were determined by direct fluorometric titration as described in Findlay et al. (1995b). Approximately 5 μM peptide (20 μM for the FW10 peptide) in 25 mM Tris, 100 mM KCl, 1 mM $CaCl_2$, pH 7.5, at 30 °C was titrated with small aliquots of concentrated protein solution (calmodulin or TR2C) and the fluorescence emission intensity at 332 (or 334) nm was recorded (excitation wavelength 280 or 290 nm). Measurements were made in UV transmitting plastic cuvettes using a SPEX Fluoromax fluorimeter with excitation and emission band widths of 1.7 and 5 nm, respectively. At least three independent determinations were performed and the average values for K_d (derived from a least-squares fitting procedure) are reported with standard deviations. The affinity of the FW10 peptide for calmodulin was also determined by a near-UV CD titration in which 225 μM calmodulin in 25 mM Tris, 100 mM KCl, 1 mM $CaCl_2$, pH 7.5, was titrated with aliquots of a concentrated peptide solution and the CD intensity at 279 nm was measured. The free peptide has negligible CD at 279 nm.

CD measurements

CD spectra were recorded in fused silica cuvettes using a Jasco J-600 spectropolarimeter. The measurements were made at room temperature in 25 mM Tris, 100 mM KCl, 1 mM $CaCl_2$, pH 7.5. Near-UV CD spectra (250–340 nm) were measured using 10-mm cuvettes with peptide/protein concentrations in the range 40–60 μM. Far-UV CD spectra (205–260 nm) were measured using 10 mm cuvettes with peptide/protein concentrations in the range 4–8 μM (at a peptide to protein ratio of 1:1). The combination of a long pathlength and relatively high protein concentrations for the far-UV measurements restricted the accessible wavelength range, but gave a large signal and therefore enabled accurate determinations of relatively small changes in CD intensity. For each sample, eight scans were averaged, the baseline subtracted, and a small degree of numerical smoothing applied. CD intensities were calculated using the molar concentration of peptide or protein ($\Delta\epsilon_M$) rather than on a per residue basis ($\Delta\epsilon_{MRW} = \Delta\epsilon_M/N_{res}$) in order to facilitate direct comparison of free proteins, peptides, and protein:peptide complexes involving different total numbers of peptide residues, N_{res}. We have used measurements of $\Delta\Delta\epsilon_M$ (222 nm) (calculated as $\Delta\epsilon_M$ for the protein/peptide complex minus $\Delta\epsilon_M$ for the free protein) to estimate the number of peptide residues adopting a helical conformation in the complex (N_H) using the formula:

$$N_H = (\Delta\Delta\epsilon_M\,(222\text{ nm}) - 0.194N)/(\Delta\epsilon^H_{MRW}\,(222\text{ nm}) - 0.194),$$

where $\Delta\epsilon^H_{MRW}$ (222 nm) = 12.122(1 − 2.5/N) is the signal expected for a completely helical peptide with N peptide bonds (Scholtz et al., 1991).

Stopped-flow measurements

All kinetic experiments were performed on a Hi-Tech SF61-MX stopped-flow spectrophotometer operated in fluorescence mode. The temperature was maintained at 30 °C and the buffer was 25 mM Tris, 100 mM KCl, pH 7.5. In experiments using EGTA as the calcium chelator, the fluorescence of the peptide tryptophan was monitored using an excitation wavelength of 280 nm with an emission cut-on filter of 305 nm. Alternatively, the fluorescence of Quin 2 was monitored using an excitation wavelength of 334 nm with an emission cut-on filter of 370 nm. The dead time of the instrument is of the order of 3 ms at a drive pressure of about 4 bar (J.F. Eccleston, pers. comm.). Fluores-

cence signals were recorded following stopped-flow mixing of typically 4 μM Ca_2-TR2C (or Ca_4-CaM) plus the required concentration of peptide and 25 μM free calcium with an equal volume of either 10 mM EGTA or 90 μM Quin 2. At least eight traces were recorded for each mixture in each experiment and at least three independent experiments were performed for each combination of complex and chelator. The individual traces were analyzed using the Hi-Tech software. A single exponential fit was adequate (as judged by inspection of χ^2 values and residuals) except in the case of dissociation of Ca_4-CaM-WFF with Quin 2, where a two-exponential function was used. Computer simulations were performed using the program KSIM and analyzed using the program KFIT. These programs were kindly provided by N. Millar.

Calcium-binding studies

Stoichiometric calcium-binding constants (K_1-K_4 for calmodulin or K_1 and K_2 for TR1C and TR2C) were determined from calcium titrations performed in the presence of different peptides, using the chromophoric calcium chelators, 5,5′-Br_2BAPTA or Quin 2 (for CaM plus the WFF peptide and for TR2C plus the WFF peptide), as described by Linse et al. (1988, 1991a) and Waltersson et al. (1993). Measurements were performed at 20 °C in 10 mM Tris, 100 mM KCl, pH 8; under these conditions, the calcium-binding constants of 5,5′-Br_2BAPTA and Quin 2 were found to be 5.7×10^5 M^{-1} and 1.1×10^7 M^{-1}, respectively (cf. 6.3×10^5 M^{-1} and 1.2×10^7 M^{-1}, respectively, reported by Linse et al. [1991b] under similar buffer conditions). The peptide to protein ratio was ≈5:1 for experiments with the WF10 peptide and ≈4:1 for those with the WFF peptide. For CaM plus the WF10 peptide, some experiments were also performed at a peptide:protein ratio of ≈12:1. At least three separate titrations were performed on each protein sample and the values for the individual binding constants (K_1-K_4 or K_1 and K_2) were obtained from least-squares fits directly to the experimentally observed titration curves as recommended by Linse et al. (1991a). As noted by Linse et al. (1991a) and by Porumb (1994), the values of $\log(K_1 K_2)$ and $\log(K_3 K_4)$ are better determined than the individual $\log(K_i)$ values.

Acknowledgments

We thank Peter Fletcher (N.I.M.R.) for the synthesis and purification of the peptides used in this study.

References

Babu YS, Bugg CE, Cook WJ. 1988. Structure of calmodulin refined at 2.2 Å resolution. *J Mol Biol 204*:191–204.

Babu YS, Sack JS, Greenhough TJ, Bugg CE, Means AR, Cook WJ. 1985. Three-dimensional structure of calmodulin. *Nature 315*:37–40.

Ban C, Ramakrishnan B, Ling KY, Kung C, Sundaralingam M. 1994. Structure of the recombinant *Paramecium tetraurelia* calmodulin at 1.68 Å resolution. *Acta Crystallogr D 50*:50–63.

Crivici A, Ikura M. 1995. Molecular and structural basis of target recognition by calmodulin. *Annu Rev Biophys Biomol Struct 24*:85–116.

Findlay WA, Gradwell MJ, Bayley PM. 1995a. Role of the N-terminal region of the skeletal muscle myosin light chain kinase target sequence in its interaction with calmodulin. *Protein Sci 4*:2375–2382.

Findlay WA, Martin SR, Beckingham K, Bayley PM. 1995b. Recovery of native structure by calcium binding site mutants of calmodulin upon binding of sk-MLCK target peptides. *Biochemistry 34*:2087–2094.

Finn BE, Evenäs J, Drakenberg T, Waltho JP, Thulin E, Forsén S. 1995. Calcium-induced structural changes and domain autonomy in calmodulin. *Nature Struct Biol 2*:777–783.

Gao ZH, Krebs J, VanBerkum MFA, Tang WJ, Maune JF, Means AR, Stull JT, Beckingham K. 1993. Activation of four enzymes by two series of calmodulin mutants with point mutations in individual Ca^{2+} binding sites. *J Biol Chem 268*:20096–20104.

Gill SC, von Hippel PH. 1989. Calculation of protein extinction coefficients from amino acid sequence data. *Anal Biochem 182*:319–326.

Gough AH, Taylor DL. 1993. Fluorescence anisotropy imaging microscopy maps calmodulin binding during cellular contraction and locomotion. *J Cell Biol 121*:1095–1107.

Guerini D, Krebs J, Carafoli E. 1984. Stimulation of the purified erythrocyte Ca^{2+}-ATPase by tryptic fragments of calmodulin. *J Biol Chem 259*:15172–15177.

Ikura M, Clore GM, Gronenborn AM, Zhu G, Klee CB, Bax A. 1992. Solution structure of a calmodulin-target peptide complex by multidimensional NMR. *Science 256*:632–638.

Ikura M, Kay LE, Krinks M, Bax A. 1991. Triple-resonance multidimensional NMR study of calmodulin complexed with the binding domain of skeletal muscle myosin light chain kinase: Indication of a conformational change in the central helix. *Biochemistry 30*:5498–5504.

Johnson JD, Snyder C, Walsh M, Flynn M. 1996. Effects of myosin light chain kinase and peptides on Ca^{2+} exchange with the N- and C-terminal Ca^{2+} binding sites of calmodulin. *J Biol Chem 271*:761–767.

Klee CB. 1977. Conformational transition accompanying the binding of Ca^{2+} to the protein activator of 3′,5′-cyclic adenosine mono-phosphate phosphodiesterase. *Biochemistry 16*:1017–1024.

Klee CB. 1988. Interaction of calmodulin with Ca^{2+} and target proteins. *Mol Asp Cell Regul 5*:35–56.

Kuboniwa H, Tjandra N, Grzesiek S, Ren H, Klee CB, Bax A. 1995. Solution structure of calcium-free calmodulin. *Nature Struct Biol 2*:768–776.

Linse S, Brodin P, Johansson C, Thulin E, Grundström T, Forsén S. 1988. The role of surface charges in ion binding. *Nature 335*:651–652.

Linse S, Helmersson A, Forsén S. 1991a. Calcium binding to calmodulin and its globular domains. *J Biol Chem 266*:8050–8054.

Linse S, Johansson C, Brodin P, Grundström T, Drakenberg T, Forsén S. 1991b. Electrostatic contributions to the binding of Ca^{2+} in calbindin D_{9k}. *Biochemistry 30*:154–162.

Luby-Phelps K, Hori M, Phelps JM, Won D. 1995. Ca^{2+}-regulated dynamic compartmentalization of calmodulin in living smooth muscle cells. *J Biol Chem 270*:21532–21538.

Martin SR, Maune JF, Beckingham K, Bayley PM. 1992. Stopped-flow studies of calcium dissociation from calcium-binding-site mutants of *Drosophila melanogaster* calmodulin. *Eur J Biochem 205*:1107–1114.

Martin SR, Bayley PM, Brown SE, Porumb T, Zhang M, Ikura M. 1996. Spectroscopic characterization of a high affinity calmodulin-target peptide hybrid molecule. *Biochemistry 35*:3508–3517.

Maulet Y, Cox JA. 1983. Structural changes in melittin and calmodulin upon complex formation and their modulation by calcium. *Biochemistry 22*: 5680–5686.

Maune JF, Klee CB, Beckingham K. 1992. Ca^{2+} binding and conformational change in two series of point mutations to the individual Ca^{2+}-binding sites of calmodulin. *J Biol Chem 267*:5286–5295.

Meador WE, Means AR, Quiocho FA. 1992. Target enzyme recognition by calmodulin: 2.4 Å structure of a calmodulin-peptide complex. *Science 257*:1251–1255.

Meador WE, Means AR, Quiocho FA. 1993. Modulation of calmodulin plasticity in molecular recognition on the basis of X-ray structures. *Science 262*:1718–1721.

Newton DL, Oldewurtel MD, Krinks MH, Shiloach J, Klee CB. 1984. Agonist and antagonist properties of calmodulin fragments. *J Biol Chem 259*:4419–4426.

Olwin BR, Storm DT. 1985. Calcium binding to complexes of calmodulin and calmodulin binding proteins. *Biochemistry 24*:8081–8086.

O'Neil KT, DeGrado WF. 1990. How calmodulin binds its targets: Sequence independent recognition of amphiphilic alpha-helices. *Trends Biochem Sci 15*:59–64.

Persechini A, McMillan K, Leakey P. 1994. Activation of myosin light chain kinase and nitric oxide synthase activities by calmodulin fragments. *J Biol Chem 269*:16148–16154.

Persechini A, White HD, Gansz KJ. 1996. Different mechanisms for Ca^{2+} dissociation from complexes of calmodulin with nitric oxide synthase or myosin light chain kinase. *J Biol Chem 271*:62–67.

Porumb T. 1994. Determination of calcium binding constants by flow dialysis. *Anal Biochem 220*:227–237.

Rao ST, Wu S, Satyshur KA, Ling KY, Kung C, Sundaralingam M. 1993. Structure of *Paramecium tetraurelia* calmodulin at 1.8 Å resolution. *Protein Sci 2*:436–447.

Scholtz JM, Qian H, York EJ, Stewart JM, Baldwin RL. 1991. Parameters of helix-coil transition theory for alanine-based peptides of varying lengths in water. *Biopolymers 31*:1463–1470.

Sekharudu CY, Sundaralingam M. 1993. A model for the calmodulin-peptide complex based on the troponin C crystal packing and its similarity to the NMR structure of the calmodulin-myosin light chain kinase peptide complex. *Protein Sci 2*:620-625.

Strynadka NCJ, James MNG. 1990. Model for the interaction of amphiphilic helices with troponin C and calmodulin. *Proteins Struct Funct Genet 7*:234-248.

Taylor DA, Sack JS, Maune JF, Beckingham K, Quiocho FA. 1991. Structure of recombinant calmodulin from *Drosophila melanogaster* refined at 2.2 Å resolution. *J Biol Chem 266*:21375-21380.

Urbauer JL, Short JH, Dow LK, Wand AJ. 1995. Structural analysis of a novel interaction by calmodulin: High-affinity binding of a peptide in the absence of calcium. *Biochemistry 34*:8099-8109.

Waltersson Y, Linse S, Brodin P, Grundström T. 1993. Mutational effects on the cooperativity of Ca^{2+} binding in calmodulin. *Biochemistry 32*:7866-7871.

Yazawa M, Ikura M, Hikichi K, Ying L, Yagi K. 1987. Communication between two globular domains of calmodulin in the presence of mastoparan or caldesmon fragment. Ca^{2+} binding and ^1H NMR. *J Biol Chem 262*:10951-10954.

Yazawa M, Vorherr T, James P, Carafoli E, Yagi K. 1992. Binding of calcium by calmodulin: Influence of the calmodulin binding domain of the plasma membrane calcium pump. *Biochemistry 31*:3171-3176.

Zhang M, Tanaka T, Ikura M. 1995. Calcium-induced conformational transition revealed by the solution structure of apo calmodulin. *Nature Struct Biol 2*:758-767.